Electronic structure of three-dimensional superlattices subject to tilted magnetic fields

N. A. Goncharuk, L. Smrčka, J. Kučera, and K. Výborný*
Institute of Physics, Academy of Science of the Czech Republic, Cukrovarnická 10, 162 53 Praha 6, Czech Republic
(Received 10 September 2004; published 20 May 2005)

A full quantum-mechanical description of electrons moving in three-dimensional structures with unidirectional periodic modulation subject to tilted magnetic fields requires an extensive numerical calculation. To understand magneto-oscillations in such systems it is in many cases sufficient to use the quasiclassical approach, in which the zero-magnetic-field Fermi surface is considered as a magnetic-field-independent rigid body in $\vec{k}$ space and periods of oscillations are related to extremal cross sections of the Fermi surface cut by planes perpendicular to the magnetic-field direction. We point out cases where the quasiclassical treatment fails and propose a simple tight-binding fully-quantum-mechanical model of the superlattice electronic structure.

DOI: 10.1103/PhysRevB.71.195318 PACS number(s): 73.63.Hs, 03.65.Sq

I. INTRODUCTION

Esaki and Tsu predicted Bloch oscillations in semiconductor superlattices in 1970,[1] and since then extensive studies of electron dynamics in these structures have been carried out. A review of research before 1987 was given by Mann,[2] who also discussed the quantization of band structure by a magnetic field parallel to the layers.

Presently, various aspects of the superlattice electronic properties are being investigated.

In quasi-two-dimensional (quasi-2D) layered organic conductors two distinct fundamental concepts of electron interlayer transport are considered: the coherent and incoherent. A comparison of both approaches was presented by McKenzie and Moses.[3,4] It has been demonstrated that the dependence of the interlayer magnetoresistance in the aforementioned natural structures on the direction of the magnetic field is identical for both models except for the case of a field almost parallel to the layers, when Yamaji oscillations[5] can occur. An explanation of magnetoresistance angular effects (Yamaji oscillations) observed in layered organic conductors has been given in the framework of the incoherent model of interlayer coupling in anisotropic multilayer systems.[6–8]

In semiconductor superlattices, the band profile of which is formed by a periodic sequence of quantum wells, the general belief is that electron motion along the growth direction is coherent and governed by the Bloch theorem. As a result, the electrons can move freely parallel to the plane of wells and their motion in the growth direction is described by minibands.

Here we consider short-period superlattices with only the lowest electron miniband occupied. In such a case, the superlattice electronic structure is close to a 3D electron system when the Fermi energy E_F lies below the top of the miniband and a Fermi surface forms a closed oval in the first Brillouin zone. When the Fermi energy coincides with the top of the miniband, the Fermi surface consists of a chain of stretched ovals "kissing" on Brillouin zone borders in the repeated zone scheme. For Fermi energies lying above the top, the Fermi surface is open and acquires the form of a corrugated cylinder. In the limiting case of impenetrable barriers the miniband width is reduced to zero and the superlattice is converted into multiple 2D electron layers. We also limit ourselves to investigation of electron structure magneto-oscillations and will not describe a specific property as magnetization (de Haas–van Alphen oscillations) or magnetoresistance (Shubnikov–de Haas oscillations).

To distinguish between 2D and 3D electron systems in superlattices, tilted magnetic fields $\vec{B}$ are used. In 3D systems the magneto-oscillations are observed for an arbitrary magnetic-field orientation, whereas in 2D systems the oscillations are determined only by a perpendicular field component B_z and disappear in the in-plane fields B_y. The tilted-magnetic-field configuration was used, e.g., to confirm the 3D nature of a semiconductor superlattice on which the existence of the quantum Hall effect in 3D structures was proved.[9]

The quasiclassical approach to the interpretation of magnetotransport experiments relies on the Onsager-Lifshitz quantization rule.[10,11] The theory states that magneto-oscillations are periodic in $1/B$ and the period of oscillations is determined by the extremal cross sections of the Fermi surface perpendicular to the direction of the applied magnetic fields. A number of extremal cross sections can be examined and the shape of the 3D Fermi surface reconstructed by tilting the sample in the magnetic field. The quasiclassical approach is also employed in studies of chaos associated with instability of electron orbits in the presence of a tilted magnetic field.[12–15]

The theory of magnetic breakdown[16–18] goes beyond the quasiclassical approximation by taking into account tunneling between eigenstates evaluated quasiclassically (by the WKB method); i.e., it is implicitly assumed that the states with high quantum numbers are involved.

The experimental evidence of deviations from the quasiclassical interpretation of data measured in tilted magnetic fields on semiconductor superlattices has been reported in Refs. 19–22. The reason is attributed to the in-plane component which is supposed to reduce the tunneling of electrons between wells when their separation is comparable with the in-plane magnetic-field length $l_y = \sqrt{\hbar/|e|B_y}$, as first proposed by Dingle[23] in 1978.

We will study this problem theoretically using a simple tight-binding, fully-quantum-mechanical model of the super-

lattice electronic structure in which the generally three-dimensional Schrödinger equation reduces to a one-dimensional differential equation.

Our approach is an extension of the model developed in 1992 by Hu and MacDonald[24] for electron bilayers subject to tilted magnetic fields, which has been many times successfully applied to a semiquantitative interpretation of the experimental data since then. Two basic approximations are employed: (i) The electron layers confined in quantum wells are strictly two-dimensional; i.e., there is no influence of the magnetic-field in-plane component on the individual layer. (ii) The barrier width and barrier height are represented by a single coupling parameter t. The problem is thus characterized by two parameters: the hopping integral t and the interlayer distance d_z.

In Sec. II we briefly summarize the textbook results (obtained with the aid of the above model) for the electronic structure of short-period superlattices in zero magnetic field. The discussion of the electronic structure in tilted magnetic fields is opened in Sec. III A by a presentation of the quasiclassical results in a form appropriate for comparison with the subsequent quantum-mechanical treatment in Sec. III B, which represents the central part of this paper. Section IV is devoted to the case of strictly in-plane magnetic fields not covered by the previous discussion. Numerical results are offered in Sec. V followed by concluding remarks in Sec. VI.

II. TIGHT-BINDING MINIBAND

A tight-binding model of minibands in 3D superlattices can be found, e.g., in Ref. 25. In this model, a superlattice is formed by a periodic sequence of quantum wells separated by barriers, with the potential energy $V(z)$ written as a sum of potential energies $V_b(z)$ of individual wells,

$$V(z) = \sum_j V_b(z - Z_j). \tag{1}$$

Here $Z_j = jd_z$, j is an integer, and d_z is a period of the superlattice. The z-dependent part of the Hamiltonian, H_z, then reads

$$H_z = \frac{p_z^2}{2m} + V(z). \tag{2}$$

For narrow wells we considered only the lowest electron miniband of the superlattice. Only the ground states $|\chi_b(z-Z_j)\rangle$ of individual wells enter our model. Their eigenenergies are taken as an origin of the energy scale. The eigenenergies of excited states are assumed to lie well above them and their presence is neglected.

In such structures the plane wave $\exp(ik_x x + ik_y y)$ describes electrons moving in the xy plane; the electron motion in the z direction is mediated by tunneling through the barriers between wells. A wave function $\chi_{k_z}(z)$ describing the miniband is the Bloch sum

$$\chi_{k_z}(z) = \sum_j e^{ik_z Z_j} \chi_b(z - Z_j). \tag{3}$$

The diagonal matrix elements of H_z are equal to zero in the basis of the ground states $|\chi_{b,j}\rangle \equiv |\chi_b(z-Z_j)\rangle$,

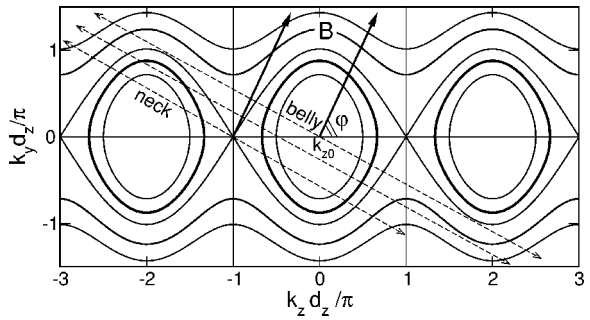

FIG. 1. Fermi surfaces of a superlattice plotted for Fermi energies lying 5 meV, 7.5 meV, 10 meV, 15 meV, and 20 meV above the miniband bottom. The tilt angle φ is 65°.

$\langle \chi_{b,j}|H_z|\chi_{b,j}\rangle = 0$. Only the hopping integrals $\langle \chi_{b,i}|V(z)|\chi_{b,j}\rangle = -t\delta_{j,i\pm1}$ are nonzero if we assume the nearest-neighbor interaction between the individual wells. As the hopping integrals are negative, t is a positive constant; i.e., in our notation $t = |t|$.

The matrix equation which determines the z-dependent part of the eigenenergies reads

$$\langle \chi_b(z - Z_j)|E - H_z|\chi_{k_z}(z)\rangle = 0. \tag{4}$$

The resulting dispersion relation $E(k_z)$ of a miniband has a simple cosine form

$$E(k_z) = -2t\cos(k_z d_z), \tag{5}$$

which depends on two parameters t and d_z. Note that the eigenfunctions $\chi_{k_z}(z)$, described by Eq. (3), are fully determined by the superlattice translation symmetry.

The energy spectrum of the 3D electron motion is composed of $E(k_z)$ and the energy of the free motion in the xy plane:

$$E(\vec{k}) = \frac{\hbar^2}{2m}(k_x^2 + k_y^2) - 2t\cos(k_z d_z). \tag{6}$$

The period of the superlattice d_z determines the size of the Brillouin zone, defined by $-\pi/d_z < k_z < \pi/d_z$. For the Fermi energy in the range of miniband energies, $-2t < E_F < 2t$, the Fermi surface has a closed semielliptic shape; for $E_F > 2t$, it is an open corrugated cylinder. Examples of constant energy surfaces are shown in Fig. 1 for a superlattice with the period $d_z = 24$ nm, miniband width $4t = 10$ meV, and electron effective mass $m = 0.067m_0$. (These parameter values will be maintained through out the whole paper unless stated otherwise.) With vanishing t, the system is transformed into a sequence of independent 2D electron layers and the Fermi surface becomes a smooth cylinder for any E_F.

III. TILTED MAGNETIC FIELDS

A. Quasiclassical approach

The standard quasiclassical approach to the electronic structure of superlattices in tilted magnetic fields and to the interpretation of related experiments is based on the Onsager-Lifshitz quantization rule

$$A_k = \frac{2\pi|e|B}{\hbar}\left(n+\frac{1}{2}\right), \tag{7}$$

where A_k is an area of the extremal cross section of the Fermi surface, perpendicular to the direction of the applied magnetic field $\vec{B}$. The plane perpendicular to $\vec{B}$, which cuts the k_z axes at $k_z = k_{z0}$, is described by

$$k_z = \frac{B_y}{B_z}k_y - k_{z0}. \tag{8}$$

There are two extremal cross sections: $k_{z0} = \pi/d_z$ corresponds to the "neck" orbit and $k_{z0} = 0$ to the "belly" orbit. In real space, the electrons move along the orbits which have the same shapes as the contours of the cross sections, but are rotated by 90° and scaled by a factor $\hbar/|e|B$.

It follows from Eq. (7) that, e.g., the magneto-oscillations are periodic in $1/B$ with the periods determined by A_k.

Here we rewrite the Onsager-Lifshitz rule in a form which employs projections $A_{k,z}$ of extremal cross sections. The reason is that this form [of course equivalent to Eq. (7)] is more appropriate for a comparison with the quantum-mechanical treatment described in the next section.

Let us denote by φ the angle between the growth direction and the direction of the magnetic field; then, $\vec{B} \equiv (0, B\sin\varphi, B\cos\varphi)$. Multiplication of Eq. (7) by $\cos\varphi$ leads to the expression

$$A_{k,z} = \frac{2\pi|e|B_z}{\hbar}\left(n+\frac{1}{2}\right), \tag{9}$$

in which the total field B was replaced by the component B_z and the cross-section area A_k of a Fermi surface by its projection to the plane $k_z = 0$, denoted by $A_{k,z}$. Similarly, multiplication of Eq. (7) by $\sin\varphi$ leads to the relation between the component B_y and the projection $A_{k,y}$ of A_k to the plane $k_y = 0$.

With the energy spectrum given by Eq. (6), the projection $A_{k,z}$ of the cross sections to the plane $z = 0$ can be written as

$$A_{k,z} = \frac{\sqrt{2m}}{\hbar} 2 \int \sqrt{E - \frac{\hbar^2 k_y^2}{2m} + 2t\cos(k_y d_y - k_{z0} d_z)}\, dk_y, \tag{10}$$

where $d_y = (B_y/B_z)d_z$.

Examples of projections $A_{k,y}$ corresponding to "belly" and "neck" cross sections of the corrugated cylinder are shown in Fig. 2. In that case two periods of magneto-oscillations exist. The contribution of orbits corresponding to k_{z0} between $-\pi/d_z$ and π/d_z to the oscillation amplitude is in general weaker, except for special cases of "extended" orbits for certain shapes of the Fermi surfaces and tilt angles. Note that a sudden step of the cross-section area, shown in Fig. 2 for a general k_{z0}, can occur also for the extremal "belly" position, if the field is slightly tilted from 65° towards the perpendicular field configuration, as obvious from an inspection of Fig. 1.

A single period corresponds to the Fermi surface formed by disconnected ovals. For independent electron layers (a smooth Fermi cylinder), Eq. (7) yields the energy spectrum

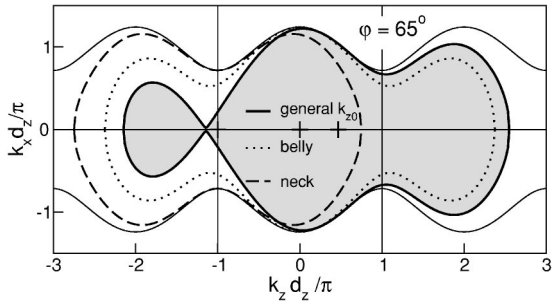

FIG. 2. Projections $A_{k,y}$ of three cross sections of the corrugated cylinder corresponding to $E_F = 15$ meV (see Fig. 1). Except for the "belly" and "neck" positions a general k_{z0} is considered, close to the critical value for which the sudden drop of the area occurs.

$E_n = \hbar\omega_z(n+\frac{1}{2})$, where $\omega_z = |e|B_z/m$, for any tilt angle. In that case the "belly" and "neck" areas are identical and only one oscillation period exists.

B. Quantum-mechanical approach

The simple tight-binding model described in Sec. II can be generalized for the case of magnetic fields of arbitrary magnitude and orientation.

Let us consider the superlattice subjected to a tilted magnetic field $\vec{B} \equiv (0, B_y, B_z)$ given by the vector potential $\vec{A} = (B_y z - B_z y, 0, 0)$. The 3D Hamiltonian H of such a system,

$$H = \frac{1}{2m}(\vec{p} - e\vec{A})^2 + V(z), \tag{11}$$

depends on the variable x only through the momentum component p_x and, consequently, the corresponding 3D wave function can be written in the form $\exp(ik_x x)\Phi(y,z)$. The function $\Phi(y,z)$ is the solution to the 2D Schrödinger equation with the Hamiltonian

$$H_{y,z} = \frac{p_y^2 + p_z^2}{2m} + \frac{1}{2m}[\hbar k_x + |e|(B_y z - B_z y)]^2 + V(z). \tag{12}$$

This expression describes a linear array of quantum dots with the minima of their potential energy at cross sections of the lines

$$\hbar k_x + |e|(B_y z - B_z y) = 0,$$

$$z = Z_j, \tag{13}$$

as shown in Fig. 3. The coordinates of minima are given by $\vec{R}_j = j\vec{d}$, where vector $\vec{d} \equiv (d_y, d_z)$ and $d_y = (B_y/B_z)d_z$. The distance between the two minima is $d = \sqrt{d_y^2 + d_z^2}$.

The eigenenergies of the corresponding Schrödinger equation are degenerated in k_x; the resulting k_x degeneracy is $|e|B_z/h$. The choice of k_x means only an unessential shift of the origin of the coordinate y or z, and we can set $k_x = 0$ without lost of generality.

We further assume, in agreement with Hu and MacDonald,[24] that the electron in an isolated well is still described by $\chi_b(z - Z_j)$, as in the zero-magnetic-field case.

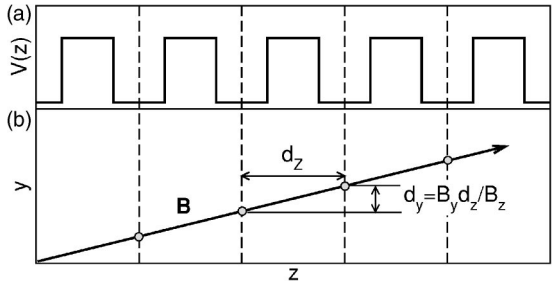

FIG. 3. (a) The schematic view of the superlattice potential. (b) The coordinates of minima of the "electromagnetic" confining potential. An electron is bound by $V_b(z-Z_j)$ in the z direction and by the magnetic harmonic potential $e^2(B_yZ_j-B_zy)^2/2m$ in the y direction.

The main effect caused by the application of $\vec{B}$ is the restriction of the in-plane motion of electrons in the y direction by the parabolic "magnetic" potential with the center at $y=Y_j$. Thus, the zero-field plane wave $\exp(ik_y y)$ should be replaced by a localized wave function which we denote $\phi(y-Y_j)$.

Since the Hamiltonian (12) is periodic with the period d, we can write the approximate wave function $\Phi(y,z)$ in the form of a Bloch sum

$$\Phi(y,z)=\sum_j e^{i\vec{k}\vec{R}_j}\chi_b(z-Z_j)\phi(y-Y_j), \tag{14}$$

where $\vec{k}\equiv(k_y,k_z)$ is a wave vector oriented in the $\vec{d}$ direction. The magnitude of the wave vector, $k=\sqrt{k_y^2+k_z^2}$, varies between $-\pi/d$ and π/d, the borders of the 1D Brillouin zone.

The matrix equation

$$\langle\chi_b(z-Z_j)|E-H_{y,z}|\Phi(y,z)\rangle=0 \tag{15}$$

yields a 1D Schrödinger equation from which the eigenfunctions $\phi_j=\phi(y-Y_j)$ and the corresponding eigenenergies are to be determined. Using

$$\phi(y+d_y)=\exp\left(i\frac{p_y}{\hbar}d_y\right)\phi(y), \tag{16}$$

we obtain for each j

$$\left[\frac{p_y^2}{2m}+\frac{m\omega_z^2}{2}(y-Y_j)^2-2t\cos\left(\frac{p_y}{\hbar}d_y-\vec{k}\vec{d}\right)\right]\phi_j=E\phi_j. \tag{17}$$

As these equations are independent and equivalent for all values of j, we can limit ourselves to a single equation with, e.g., $j=0$. Employing the p representation, Eq. (17) can be written as

$$\left[-\frac{m\hbar^2\omega_z^2}{2}\frac{\partial^2}{\partial p_y^2}+\frac{p_y^2}{2m}-2t\cos\left(\frac{p_y}{\hbar}d_y-\vec{k}\vec{d}\right)\right]\phi_0=E\phi_0, \tag{18}$$

where ϕ_0 is a function of p_y, $\phi_0=\phi_0(p_y)$. Thus the 3D Schrödinger equation is reduced to 1D, with the energy spectrum formed by 1D Landau subbands $E_n(\vec{k})$. This is the central result of this paper.

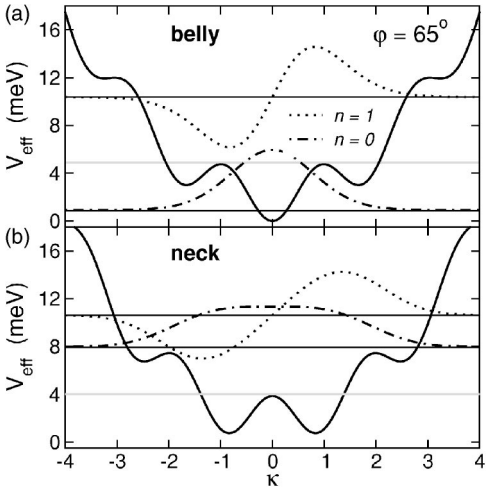

FIG. 4. The modulated parabolic well in p space for (a) the "belly" position and (b) the "neck" position of k_{z0}. Two lowest eigenstates and eigenenergies are calculated for $B_z=3$ T. The gray lines correspond to the critical parameters of quasiclassical orbits, at which the area calculated using Eq. (10) changes abruptly. The dimensionless variable κ is determined by $\hbar\kappa=\ell_z p_y$, where $\ell_z=\sqrt{\hbar/|e|B_z}$.

The parabolic well in p space modulated by the cosine potential is shown in Fig. 4 for two values of the phase factor, 0 and π. The choice $\vec{k}\cdot\vec{d}=0$ corresponds to the "belly" orbit and $\vec{k}\cdot\vec{d}=\pi$ to the "neck" orbit in quasiclassical terminology.

In principle, Eq. (18) can be solved quasiclassically (by the WKB method) or quantum mechanically. The choice of the method depends on the system parameters.

As anticipated, the quasiclassical solution leads to the expression (10). Note that the phase factor $\vec{k}\cdot\vec{d}$ can be replaced by $k_{z0}d_z$. [The projection k_{z0} of $\vec{k}$ onto the k_z axis satisfies $k_{z0}\in(-\pi/d_z,+\pi/d_z)$.] Generally, the WKB method is applicable if $\hbar\omega_z\ll 4t$ and many states below the Fermi level are occupied.

The gray lines shown in Fig. 4 denote tops of the "potential" barriers which separate the classically inaccessible regions of p_y. The magnetic breakdown theory describes tunneling between two *quasiclassical* orbits from neighboring regions.

In semiconductor superlattices $\hbar\omega_z$ becomes comparable to $4t$ in relatively weak magnetic fields. Two lowest eigenstates calculated quantum mechanically are shown in Fig. 4. The wave functions extend over several local minima of the "potential," just in opposition to requirements of the quasiclassical approximation and the magnetic breakdown theory, which clearly cannot be applied in this case.

IV. IN-PLANE MAGNETIC FIELD

The above approach fails for the case $B_z\to 0$. In an in-plane magnetic field $\vec{B}=(0,B_y,0)$ the vector potential takes the form $\vec{A}=(B_y z,0,0)$ and the one-electron Hamiltonian (12) reduces to

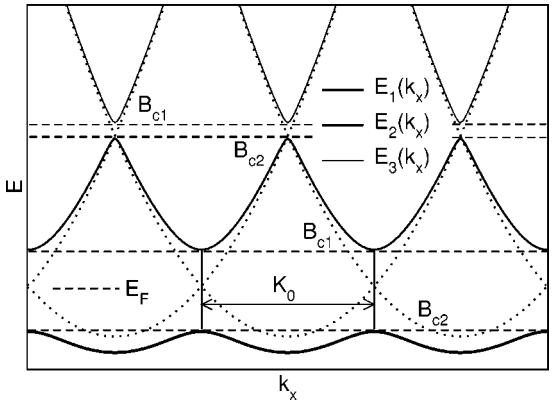

FIG. 5. The energy dispersion curves $E_n(k_x)$. The dotted lines correspond to independent 2D electron layers, $t=0$. The dashed lines denote subband boundaries.

$$H_y = \frac{p_y^2 + p_z^2}{2m} + \frac{1}{2m}(\hbar k_x + |e|B_y z)^2 + V(z). \tag{19}$$

Treating the interwell hopping in a tight-binding approximation as in Sec. III B, the Hamiltonian (19) transforms to a three-diagonal matrix with diagonal and off-diagonal elements given by

$$H_{j,j} = \frac{\hbar^2}{2m}(k_x + k_j)^2 + \frac{\hbar^2 k_y^2}{2m}, \quad H_{j,j\pm1} = -t, \tag{20}$$

where $k_j = jK_0$ is the magnetic-field-dependent wave vector with $K_0 = |e|B_y d_z/\hbar = d_z/\ell_y^2$. This is a matrix form of the Mathieu equation (see, e.g., Ref. 26).

Solving the eigenvalue problem we get a number of Landau subbbands $E_n(k_x)$ which are K_0 periodic in k_x. Then the full energy spectrum is given by

$$E_n(k_x, k_y) = E_n(k_x) + \frac{\hbar^2 k_y^2}{2m}. \tag{21}$$

The lowest subbands $E_n(k_x)$ are shown in Fig. 5. The states from neighboring layers, described by dotted parabolas, are mixed at the border of Brillouin zones where the free-electron parabolas cross. The electrons tunnel between wells near the cross points and energy gaps open there.

This is reflected in the shape of equienergetic lines $E_F = E_n(k_x, k_y)$. For large enough B_y the separation of centers, K_0, becomes larger than the diameter of the free-electron Fermi circles $2k_F$. The contours do not cross and electrons cannot tunnel at all. Note that this condition is equivalent to $d_z > 2\ell_y k_F$, proposed by Dingle[23] as mentioned in the Introduction.

With lowering the field (and smaller K_0) the Fermi contours first "kiss" on borders of Brillouin zones when E_F touches the top of the lowest Landau subband. Then they merge into an open contour and a new Fermi oval, belonging to the second subband, appears when E_F reaches its bottom, etc.

This is illustrated by dashed lines in Fig. 5. For simplicity we use fixed B_y and variable E_F, instead of the fixed Fermi energy and sweeping B_y.

Two types of critical magnetic fields (energies) can be distinguished: B_{c1} and B_{c2}. When the Fermi energy touches the bottom of a Landau subband at B_{c1}, there is a minimum in $E_n(k_x, k_y)$ and the steplike van Hove singularity appears in the density of states. The second possibility is the Fermi energy coinciding with the maximum of an $E_n(k_x)$ at B_{c2}. It corresponds to the saddle point in $E_n(k_x, k_y)$ and the logarithmic van Hove singularity results in the density of states.

V. NUMERICAL EXAMPLE

It is clearly illustrated in Fig. 4 that the quantum-mechanical regime, when only a few Landau subbands are occupied and the quasiclassical approach is not valid, can be reached in relatively weak magnetic fields for realistic parameters of superlattices. In the quasiclassical approach the electron motion in the effective "potential" should be limited by local side maxima, due to the cosine modulation. In quantum mechanics electrons can tunnel through the local barriers even if their energy is below the maxima. In principle, it is possible to describe tunneling through the barriers quasiclassically as the "magnetic breakdown," but it seems not very appropriate for states with lowest quantum numbers.

In experiments, usually the concentration of carriers is kept fixed and the magnetic field is varied. In most cases experimental data reflect the field-induced singularities of the density of states. Therefore, we concentrate in our numerical example on the evaluation of the density-of-states field dependence for a series of tilt angles. The results of both approaches will be compared.

For simplicity, we start with the analytically solvable case of perpendicular magnetic fields.

A. Perpendicular magnetic field

In the quasiclassical approximation, two extremal circular orbits, a "belly" and a "neck," can be found on the corrugated cylinder with the cross sections

$$A_{k,belly} = \pi\frac{2m}{\hbar^2}(E_F + 2t), \quad A_{k,neck} = \pi\frac{2m}{\hbar^2}(E_F - 2t). \tag{22}$$

For these orbits, the quantization condition (7) can be rewritten as

$$E_F \pm 2t = \hbar\omega_z\left(n + \frac{1}{2}\right), \tag{23}$$

which yields two periods of oscillations

$$\Delta\left(\frac{1}{B_z}\right)_{\substack{belly \\ neck}} = \frac{\hbar|e|}{m(E_F \pm 2t)}. \tag{24}$$

It follows from Eq. (24) that for the Fermi energy close to the miniband top the period of a "neck" orbit increases and reaches infinity at $E_F = 2t$. For E_F within the miniband the Fermi surface consists of disconnected ovals and only one oscillation period exists, corresponding to the "belly" orbits.

The energy spectrum obtained by a full-quantum-mechanical solution of the Schrödinger equation profits from

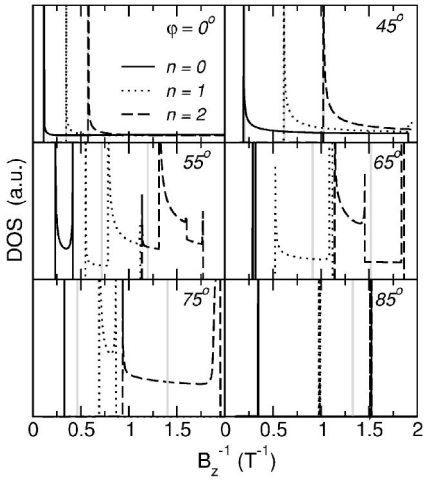

FIG. 6. The magnetic-field-dependent density of states calculated for Fermi energy 7.5 meV above the miniband bottom. First three Landau subbands are shown. The gray lines correspond to singularities calculated quasiclassically.

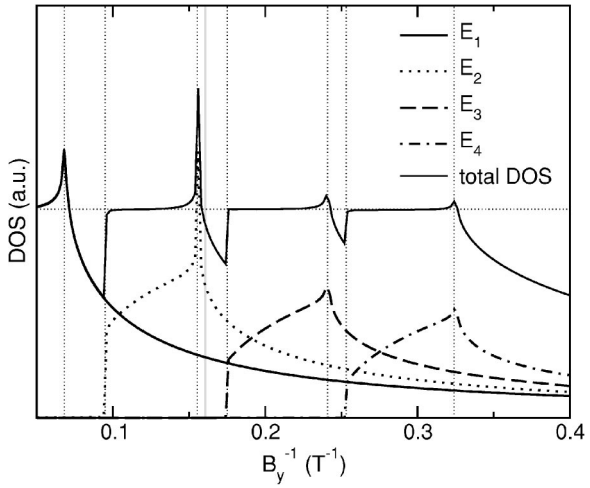

FIG. 7. The magnetic-field-dependent density of states calculated for Fermi energy 7.5 meV above the miniband bottom. The gray line corresponds to the singularity calculated quasiclassically. (Only one singularity is depicted.)

the fact that in perpendicular magnetic fields $d_y=0$. Consequently, Eq. (18) is reduced to the standard equation of free-electron motion in perpendicular magnetic fields. Landau subbands are formed by a sum of Landau energy levels and the 1D miniband, like in the zero-field case:

$$E_n(\vec{k}) = \hbar\omega_z\left(n+\frac{1}{2}\right) - 2t\cos(k_z d_z). \tag{25}$$

Due to the periodic potential, the Landau levels are broadened into Landau subbands.

The corresponding density of states per layer, $g(E)$, can be evaluated analytically and reads

$$g(E) = \frac{|e|B_z}{h}\frac{1}{\pi}\sum_n \frac{1}{\sqrt{4t^2 - \left[E-\hbar\omega_z\left(n+\frac{1}{2}\right)\right]^2}}. \tag{26}$$

Two van Hove singularities (of the type $1/\sqrt{E}$) are due to the maximum and minimum of the Landau subband at the borders of the Brillouin zone. Their positions on the energy axis are given by Eq. (23); i.e., they correspond to the extremal "belly" and "neck" orbits obtained quasiclassically. At fixed Fermi energy, these extrema define two oscillation periods in the B_z dependence of the density of states.

B. Tilted magnetic fields

To stress the difference between the quasiclassical and quantum-mechanical solutions, we shall consider a superlattice with the closed semielliptic Fermi surface, presented in Fig. 1.

In such a case the quasiclassical solution leads to single-period oscillations, with the period depending on the area of the "belly" extremal cross sections, which vary with the tilt angle. With the distance of nonextremal to extremal orbits their contribution to the oscillation amplitude smoothly vanishes.

As the largest difference between the quasiclassical and quantum-mechanical approaches is expected for lowest eigenenergies, we present in Fig. 6 the density of states of three lowest Landau subbands calculated for the fixed E_F as a function of $1/B_z$. To study the increasing influence of the in-plane field component B_y, the tilt angle is varied from the perpendicular position, $\varphi=0$, towards the in-plane field configuration. In addition to the curves obtained from the quantum-mechanical solution of Eq. (18), the position of the quasiclassical "belly" orbits is shown.

As mentioned above, both methods yield exactly the same results in the perpendicular magnetic-field orientation, $\varphi=0$, and only small deviations of singularities corresponding to the "belly" orbits are found for angles up to 45°. At 45° marked deviations appear. The "neck" singularity returns to the first Landau subband; i.e., its width becomes finite. Moreover, an additional singularity occurs in the second Landau subband.

Above 45° the two solutions are completely different. While the period of quasiclassical oscillations monotonously increases with the decreasing area of the "belly" cross section, the quantum-mechanical solution exhibits new features. Two singularities in the first Landau subband become closer as φ grows; the width of the subband shrinks and around 65° it remains at a level.

In the second Landau subband, an additional singularity shows up besides the "belly" and "neck" singularities which vanishes above 65°. Then also the second subband shrinks in a level.

Four singularities appear in the third subband; for higher φ their number is subsequently reduced to 3 and then 2 before the subband shrinks to a level. Obviously, the number of singularities is related to the number of nodes of the corresponding wave functions.

C. In-plane magnetic fields

For the semielliptic Fermi surface there is no difference between the in-plane and tilted magnetic field in the quasiclassical approximation. The single period of oscillations is

determined by the extremal cross section which is now in the $k_x k_z$ plane. The corresponding singularity is shown in Fig. 7 together with the density of states which results from processing the numericaly obtained eigenenergies $E_n(k_x, k_y)$. Both results show a pronounced qualitative difference.

The quasiclasical approach does not distinguish between the perpendicular and in-plane magnetic fields. It assumes that the 1D subbands attached to the quasiclassicaly calculated Landau levels are emptied by increasing the magnetic field. But this is correct only for the perpendicular field orientation.

In the quantum-mechanical picture 2D Landau subbands are emptied and instead of the van Hove singularities of $1/\sqrt{E}$ type, logarithmic and steplike singularities appear.

VI. CONCLUSIONS

In superlattices with period d_z, the in-plane magnetic-field component B_y displaces the origins of the Fermi circles of neighboring electron layers by $|e|B_y d_z/\hbar$. Above the critical field $B_{y,c}=2\hbar k_F/|e|d_z$ the Fermi circles with radii k_F cannot cross and tunneling is impossible.

The theoretical description is particularly simple for the tight-binding model of the electronic structure; the generalized Landau eigenenergies in tilted magnetic fields can be found as solutions to a one-dimensional Schrödinger equation.

The quasiclassical solution to this 1D problem yields the standard Onsager-Lifshitz rule. The full-quantum-mechanical solution is necessary to describe the 3D$\rightarrow$2D transition—i.e., the transition to a sequence of independent 2D electron layers.

ACKNOWLEDGMENTS

This work has been supported by the Grant Agency of the ASCR under Grant No. IAA1010408, by the French-Czech Project No. Barrande 2003-013-2, and by the Institutional Research Plan No. AV0Z10100521.

*Present address: Institute of Theoretical Physics, University of Hamburg, Jungiusstrasse 9, 20355 Hamburg, Germany.

[1] L. Esaki and R. Tsu, IBM J. Res. Dev. **14**, 61 (1970).
[2] J. K. Maan, Adv. Solid State Phys. **27**, 137 (1987).
[3] R. H. McKenzie and P. Moses, Phys. Rev. Lett. **81**, 4492 (1998).
[4] P. Moses and R. H. McKenzie, Phys. Rev. B **60**, 7998 (1999).
[5] K. Yamaji, J. Phys. Soc. Jpn. **58**, 1520 (1989).
[6] T. Osada, H. Nose, and M. Kuraguchi, Physica B **294-295**, 402 (2001).
[7] T. Osada, Physica E (Amsterdam) **12**, 272 (2002).
[8] T. Osada, M. Kuraguchi, K. Kobayashi, and E. Ohmichi, Physica E (Amsterdam) **18**, 200 (2003).
[9] H. L. Störmer, J. P. Eisenstein, A. C. Gossard, W. Wiegmann, and K. Baldwin, Phys. Rev. Lett. **56**, 85 (1986).
[10] L. Onsager, Philos. Mag. **43**, 1006 (1952).
[11] N. W. Ashcroft and N. D. Mermin, *Solid State Physics* (Saunders, Philadelphia, 1975), p. 368.
[12] C. R. Tench, T. M. Fromhold, S. Bujkewicz, P. B. Wilkinson, F. W. Sheard, and L. Eaves, Physica B **272**, 209 (1999).
[13] S. Bujkewicz, T. M. Fromhold, M. J. Carter, F. W. Sheard, and L. Eaves, Physica E (Amsterdam) **7**, 827 (2000).
[14] K. Kobayashi, M. Saito, E. Ohmichi, and T. Osada, Physica E (Amsterdam) **22**, 385 (2004).
[15] T. M. Fromhold, A. Patanè, S. Bujkewicz, P. B. Wilkinson, D. Fowler, D. Sherwood, S. P. Stapleton, A. A. Krokhin, L. Eaves, M. Henini, N. S. Sankeshwar, and F. W. Sheard, Nature (London) **428**, 726 (2004).
[16] M. H. Cohen and L. M. Falicov, Phys. Rev. Lett. **7**, 231 (1961).
[17] E. I. Blount, Phys. Rev. **126**, 1636 (1961).
[18] W. G. Chambers, Proc. Phys. Soc. London **82**, 181 (1964).
[19] O. Jaschinski, G. Nachtwei, J. Schoenes, P. Bönsch, and A. Schlachetzki, Physica B **251**, 873 (1998).
[20] G. Nachtwei, A. Weber, O. Jaschinski, and H. Künzel, J. Appl. Phys. **84**, 323 (1998).
[21] M. Kawamura, Ph.D. thesis, University of Tokyo, 2000, p. 31.
[22] M. Kawamura, A. Endo, S. Katsumoto, Y. Iye, C. Terakura, and S. Uji, Physica B **298**, 48 (2001).
[23] R. Dingle, Surf. Sci. **73**, 229 (1978).
[24] J. Hu and A. H. MacDonald, Phys. Rev. B **46**, 12 554 (1992).
[25] G. Bastard, *Wave Mechanics Applied to Semiconductor Heterostructures* (Monographies de Physique, Paris, 1992), p. 22.
[26] S. G. Davidson and M. Stęślicka, *Basic Theory of Surface States* (Clarendon Press, Oxford, 1992), p. 41.